



# Detection of theophylline using molecularly imprinted polymers based on thioglycolic acid-modified CdTe quantum dots

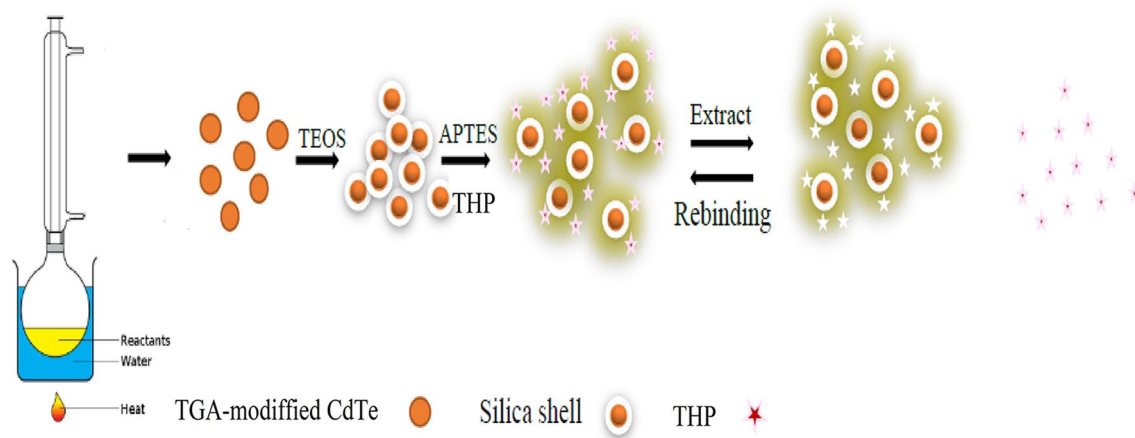
Maryam Zakery<sup>1</sup> · Ali A. Ensafi<sup>1</sup> · Behzad Rezaei<sup>1</sup>

Received: 12 July 2019 / Accepted: 20 October 2019 / Published online: 29 October 2019  
© Iranian Chemical Society 2019

## Abstract

Molecularly imprinted polymers (MIPs) and quantum dots (QDs) have been widely employed to fabricate highly sensitive and selective sensor. Here, we developed a fluorescence nanosensor based on thioglycolic acid-modified CdTe QDs that is coated with molecularly imprinted polymers for the specific detection of theophylline (THP). Initially, water-soluble thioglycolic acid-modified CdTe QDs were synthesized by refluxing method. Then, MIPs-coated QDs (MIPs-QDs) composite was produced by sol–gel process using THP as a template. Therefore, the selectivity of the molecular imprinting technique and advantages of QDs were combined. The prepared QDs and the MIPs-QDs were characterized using X-ray diffraction technique, transmission electron microscopy, dynamic light scattering, Fourier transform infrared spectroscopy, and fluorescence spectrometry. Finally, this sensing system was successfully used to detect THP in human plasma samples with recoveries of 90% to 108%. A very good linear relationship was observed between the decreasing in the fluorescence intensity of MIPs-QDs and increasing the THP concentration within concentration range of 0.14–3.05  $\mu\text{mol L}^{-1}$ , with a correlation coefficient of 0.9992 and detection limit of 0.07  $\mu\text{mol L}^{-1}$ .

## Graphic abstract



**Keywords** Theophylline · Molecularly imprinted polymers · Thioglycolic acid-modified CdTe QDs

## Introduction

In the recent years, quantum dots (QDs) as semiconductor fluorescent nanocrystals that have diameters in the range of 2 to 10 nm have been developed for using as photoluminescence probes to measure several types of compounds such

✉ Ali A. Ensafi  
Ensafi@cc.iut.ac.ir; aaensafi@gmail.com; ensafi@yahoo.com

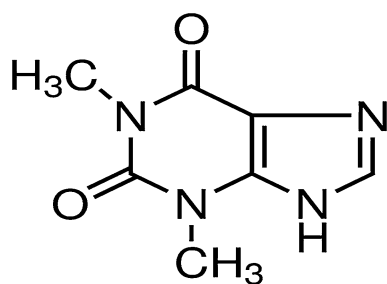
<sup>1</sup> Department of Chemistry, Isfahan University of Technology, Isfahan 84156-83111, Iran

as drugs, explosive compounds, organic dyes, and inorganic anions and cations. QDs have remarkable optical and electrical properties such as high photoluminescence intensity, high light stability, continuous absorption spectra, sharp emission band, and high resistance to photobleaching [1, 2]. Therefore, QDs have been applied as fluorescence sensors and as the core in the imprinting process for industrial and commercial applications.

Molecular imprinting is a technology of producing synthetic selective sites in polymeric matrices with the memory of template, which is complementary to the template in size, shape, and chemical functionality. Molecularly imprinting polymers (MIPs) are 3D structures whereby the template molecule is formed by growing a polymeric matrix around it. The 3D mold is capable of rebinding to the template molecule after its removal from the polymeric matrix core [3–5]. MIPs show important advantages, containing high mechanical/chemical stability, easy preparation, reusability, and inexpensive production [6–8].

Theophylline (Scheme 1) is a useful bronchodilator in cases of asthma, bronchitis, and emphysema. The plasma concentration range of 20–100 mmol L<sup>-1</sup> is useful for effective bronchodilation action, and it has toxic effect at higher concentrations. It can be lethal or lead to permanent neurological damage [9].

Different methods have been described for the determination of theophylline, including colorimetric [10], gas/liquid chromatography [11], enzyme immunoassay [12], stopped-flow fluorimetric [13], and flow injection fluorimetry [14]. Recently, advanced methods for measurement of THP have been suggested such as RNA aptamer-based gold nanoparticle sensor [15] and hand-in-hand RNA nanowire-based aptasensor [16]. The advantages of the mentioned methods were sensitivity and accuracy, although they require expensive instruments and are also time-consuming. It is important to find a fast, simple, and low-cost method with high selectivity and sensitivity for the determination of THP. The main advantages of the combination of MIPs and the modified QDs, as a simple and low-cost nanosensor for rapid detection of THP, are high selectivity and sensitivity.



**Scheme 1** The molecular structure of THP

## Experimental

### Materials

All of chemicals (except theophylline) were purchased from Sigma-Aldrich company, and they are used without any purification. Thioglycolic acid (TGA), NaBH<sub>4</sub>, CdCl<sub>2</sub>·H<sub>2</sub>O, and Na<sub>2</sub>TeO<sub>3</sub> were used for the synthesis of thioglycolic acid-modified CdTe QDs. Acetone, cyclohexane, ammonium hydroxide solution (25–28%), Triton X-100, tetraethoxysilane (TEOS), 3-aminopropyl triethoxysilane (APTES), ethanol, and acetonitrile were used for the fabrication of MIPs and NIPs. Theophylline (THP) was obtained from Sina Darou Pharmaceutical Company.

### Synthesis of thioglycolic acid-modified CdTe quantum dots

Preparation of TGA-modified CdTe QDs was carried out in accordance with technique reported in previous works [17]. Initially, TGA (0.3 mL) was dissolved in distilled water (110 mL). Then, CdCl<sub>2</sub>·H<sub>2</sub>O (0.508 g) was added to the above solution and the mixture was stirred (30 min) at room temperature. Afterward, NaBH<sub>4</sub> (1.25 g) and Na<sub>2</sub>TeO<sub>3</sub> (10 mL of 0.1 mol L<sup>-1</sup>) were sequentially added dropwise to the above mixture with stirring. Finally, the mixture was refluxed at 95 °C for 2 h. The prepared TGA-modified CdTe QDs were kept at 4 °C.

### Preparation of TGA-modified QDs-MIPs and QDs-NIPs

QDs-MIPs were successfully prepared by reverse microemulsion method [18]. Initially, 7.5 mL of cyclohexane (continuous phase) was mixed with 1.8 mL of Triton X-100 (surfactant). Then, 400 μL of TGA-modified CdTe QDs (synthesized in Sec. 2.2), 50 μL TEOS (cross-linker), and 100 μL of aqueous ammonium hydroxide solution (as a catalyst) were added to the above solution, and the mixture was stirred at room temperature for 2 h. Afterward, 5 mg of THP and 20 μL of APTES were added into the above mixture and stirred for 12 h to complete the polymerization. Then, the microemulsion was broken by adding acetone (20 mL) and it was centrifuged at 6000 rpm for 5 min. The QDs-MIPs nanocomposite was washed with ethanol/acetonitrile (80/20 v/v) until the templates are removed from the MIPs, and no template molecules can be detected by UV–Vis spectrophotometry. For the evaluation of the efficiency of the TGA-modified CdTe QDs-MIPs, non-imprinted polymers (QDs-NIPs) were simultaneously

produced without the addition of the template molecules [19].

## Fluorometric analysis

The measurement of the fluorescence intensity was carried out by a fluorescence spectrometer (Jasco FP-750-Japan). For this purpose, 3.0 mg of the MIPs TGA-modified CdTe QDs-MIP was dispersed in 3.0 mL of phosphate buffer solution (pH 7.0). Then, the fluorescence intensity ( $\lambda_{\text{ex}} = 400$  nm,  $\lambda_{\text{em}} = 533$ ) was recorded before (F0) and after (F) addition of different amounts of THP standard solution. Changes in the fluorescence intensity (F0–F) were calculated as a response function, to assess the THP concentration. Then, the values of the F0–F were plotted with respect to the different concentrations of THP.

## Sample preparation

Fresh plasma was prepared from Isfahan University of Technology Medical Center. The proteins were precipitated by trichloroacetic acid, and the upper phase was filtered through 0.45- $\mu\text{m}$  filter and diluted tenfold using phosphate buffer solution (pH 7.0). Certain volume of the standard solution of THP was spiked into the diluted plasma. Then, 300  $\mu\text{L}$  of the

spiked plasma was added into a fluorimetric cell containing the QDs-MIPs (1000 mg L<sup>-1</sup> at phosphate buffer solution, pH 7.0). The concentration of THP was computed by standard addition method.

## Result and discussion

### Characterization of QDs, QDs-MIPs, and QDs-NIPs

FT-IR spectra of TGA free and TGA-modified CdTe QDs are compared in Fig. 1A. For TGA, the peak around 2560 cm<sup>-1</sup> displays the S–H stretching vibration, whereas for the TGA-modified CdTe QDs this peak is absent and proves the formation of a covalent bond between CdTe and sulfur of TGA. As can be seen in Fig. 1A (MIPs and NIPs), the strong peaks around 1030–1080 cm<sup>-1</sup> are due to the stretching vibrations of Si–O–Si and Si–OH, whereas the peak at 790 cm<sup>-1</sup> is due to bending vibrations of the Si–O groups [17]. The IR band of the C–H stretching was observed around 2940 cm<sup>-1</sup>. The peak around 3370 cm<sup>-1</sup> corresponds to the stretching band of the N–H and displays the presence of APTES in the synthesized MIPs and NIPs. The results proved that the MIPs and NIPs effectively were synthesized on the surface of the QDs.

**Fig. 1** **A** FT-IR spectra of the TGA, TGA-modified QDs, MIPs, and NIPs; **B** The template molecule (THP) absorption spectrum (a) and fluorescence emission spectra of QDs-MIPs (b); **C** UV–Vis absorption (a) and fluorescence spectra of the TGA-modified CdTe QDs

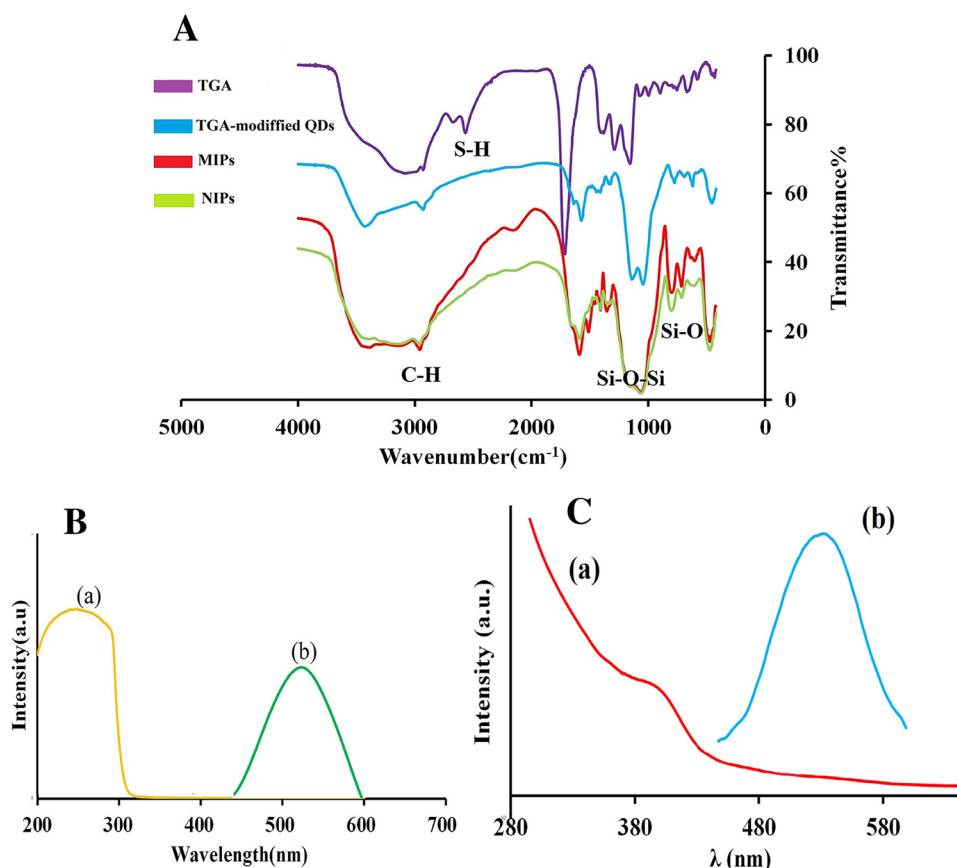


Figure 1B shows the absorption (a) and fluorescence emission spectra of QDs-MIPs (b). As displayed in Fig. 1B, there is no overlap between the THP absorption spectrum (Fig. 1B-a) and the QDs emission spectrum (Fig. 1B-b). Figure 1C shows the UV–Vis absorption (a) and fluorescence spectrum of the TGA-modified CdTe QDs. These spectra also confirm that there is no overlap between the absorption (Fig. 1C-a) and fluorescence (Fig. 1C-b) spectra of TGA-modified CdTe QDs.

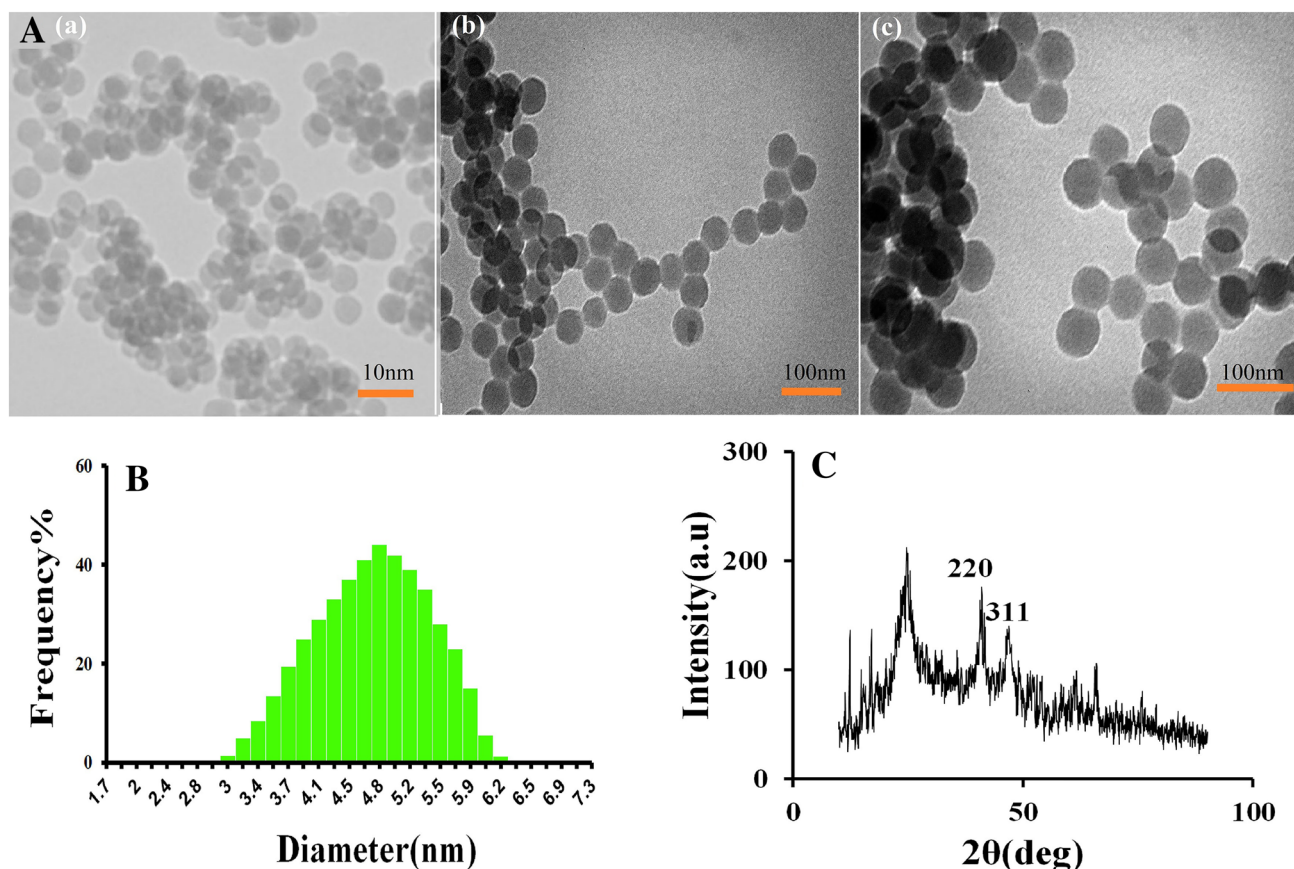
Figure 2A shows TEM images of the TGA-modified CdTe QDs (a), MIPs (b), and NIPs (c). Spherical particles are observed in the TEM images of MIPs and NIPs and are similar in their sizes. As shown in these images, the average size of the QDs and MIPs is estimated about 5 nm and 50 nm, respectively. Also, the size distribution of the QDs was determined using DLS technique. As displayed in Fig. 2B, the diameter of the QDs was estimated at around 5 nm.

Figure 2C shows the XRD pattern of the TGA-modified CdTe QDs in the  $2\theta$  range of  $10^\circ$ – $60^\circ$ . The angles of the diffractive peaks were observed at  $24.16^\circ$ ,  $40.31^\circ$ , and

$46.82^\circ$  that corresponds to the zinc blende planes of (111), (220), and (311), respectively.

## Mechanism

The MIPs were synthesized using the reverse microemulsion method [20]. Initially, the QDs should be coated with a silica shell because the silica shell increases the interactions between QDs and APTES (functional monomer) and reduces the toxicity of the QDs. Ammonium hydroxide catalyzes the hydrolysis of the TEOS (cross-linker) to silica on the surface of QDs. The MIPs were produced by copolymerization reaction using TEOS (cross-linker) and APTES in the presence of THP as a template. As displayed in Scheme 1, THP contains nitrogenous groups that interact to APTES through hydrogen bonding. The specific interactions of the THP with the imprinted cavities were followed by fluorescence spectroscopy. When THP enter into the imprinted cavities, the fluorescence intensity of the THP-MIPs clearly decreases. The charge transfers between the THP and QDs are suggested as a quenching mechanism. As displayed in Fig. 1B, there is no overlap between the THP absorption spectrum



**Fig. 2** A TEM images of (a) TGA-modified CdTe QDs (scale bar: 10 nm); (b) QDs-MIPs (scale bar: 100 nm); and (c) QDs-NIPs (scale bar: 100 nm); B DLS diagram of TGA-modified CdTe QDs; C X-ray diffraction pattern of the TGA-modified CdTe QDs

(Fig. 1B-a) and the QDs emission spectrum (Fig. 1B-b). A charge transfer occurs from conduction band of the QDs to the lowest unoccupied molecular orbital (LUMO) of the UV band of THP. Then, the excited charges tend to go back, and quenching is generated.

### Effect of pH

The effect of solution pH (4–11) on the fluorescence response of the nanosensor to THP ( $0.55 \mu\text{mol L}^{-1}$ ) was studied. The phosphate buffer solution was employed to investigate the effect of the solution pH on the sensor sensitivity. The obtained responses are indicated in Fig. 3a. As can be seen, the best possible result was obtained at pH 7.0. The sensitivity decreased in acidic or alkaline conditions. Under acidic conditions ( $\text{pH} < 7.0$ ), the hydrogen bonding strength between the APTES functional monomer group  $-\text{NH}_2$  and theophylline decreases, thereby reducing the sensitivity. In the alkaline environment, TGA molecules, that are coated on the surfaces of the quantum dots, can be ionized and therefore the energy levels of the conduction band of the quantum dots change and the charge transfer does not occur effectively. Thus the response of the sensor was decreased at  $\text{pH} > 7.0$ . Also at highly alkaline pHs, hydroxyl ions could attack the surface of the MIPs and affect the interaction between the MIPs and THP [21].

### Effect of duration time

The effect of time between adding THP ( $0.55 \mu\text{mol L}^{-1}$ ) and recording the fluorescence signal was investigated. As shown in Fig. 3b, the fluorescence intensity change ( $F_0-F$ ) increased in the initial 90 s and then remains almost constant. Therefore, 90 s was chosen as the optimal duration.

### Figures of merit

The sensitivity of the sensor toward the THP ( $0.28\text{--}3.05 \mu\text{mol L}^{-1}$ ) was investigated and compared with NIPs, as shown in Figs. 4A-a, B and 5b, respectively. The results showed that

when the THP concentration increased from 0 to  $3.05 \mu\text{mol L}^{-1}$ , the fluorescent intensity of the sensor obviously decreased while the fluorescence intensity of NIP-QDs is slightly changed. As a result, the sensor has a better sensitivity versus the MIPs-QDs. To find out the detection range, the fluorescence intensity changes of the sensor, ( $F_0-F$ ), were plotted vs. the concentration of THP (Fig. 4A-b). A very good linear relationship was observed between the decreasing in the fluorescence intensity of MIPs-QDs and increasing the THP concentration within  $0.28\text{--}3.05 \mu\text{mol L}^{-1}$  with a correlation coefficient of 0.9961 and detection limit  $0.07 \mu\text{mol L}^{-1}$  ( $\text{LOD} = \frac{Sy/x}{m}$ ,  $Sy/x = \frac{\sqrt{\sum(y_i - \hat{y}_i)^2}}{n-2}$ ).

The relative standard deviations (RSD) were calculated for three successive replicate measurement of  $0.5 \mu\text{mol L}^{-1}$  and  $1.6 \mu\text{mol L}^{-1}$  THP, as 6.8% and 3.2%, respectively.

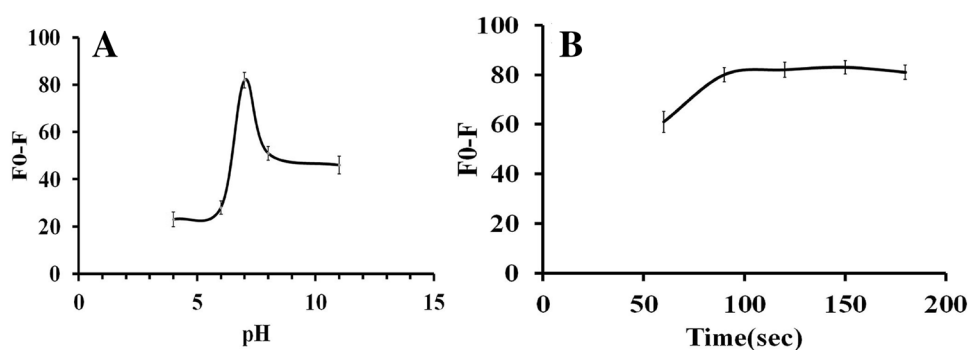
### Selectivity study

The selective recognition of the sensor was tested and compared with a bare QDs and QDs-NIPs. The common compounds in plasma such as aspartic acid, alanine, cysteine, ascorbic acid, isoleucine, glycine, NaCl, KCl,  $\text{CaCl}_2$ , and  $\text{MgCl}_2$  (all in  $1.0 \text{mmol L}^{-1}$ ) were used in order to investigate the selectivity of the sensor. As displayed in Fig. 5, the sensitivity of the sensor for the determination of THP ( $1.0 \mu\text{mol L}^{-1}$ ) is clearly better than the unmodified QDs and NIPs. Also, the sensor has the ability of specific recognition of THP than the other compounds. This is due to cavities with favorable binding sites for THP that formed in the QDs-MIPs.

### Application

To investigate the applicability of the sensor in real samples, the sensor was used to the measurement of THP in plasma samples. Recovery studies were carried out by spiking the plasma samples with various amounts of THP.

**Fig. 3** a Effect of pH on the fluorescence intensity of QDs-MIPs; b effect of time on the fluorescence intensity of QDs-MIPs



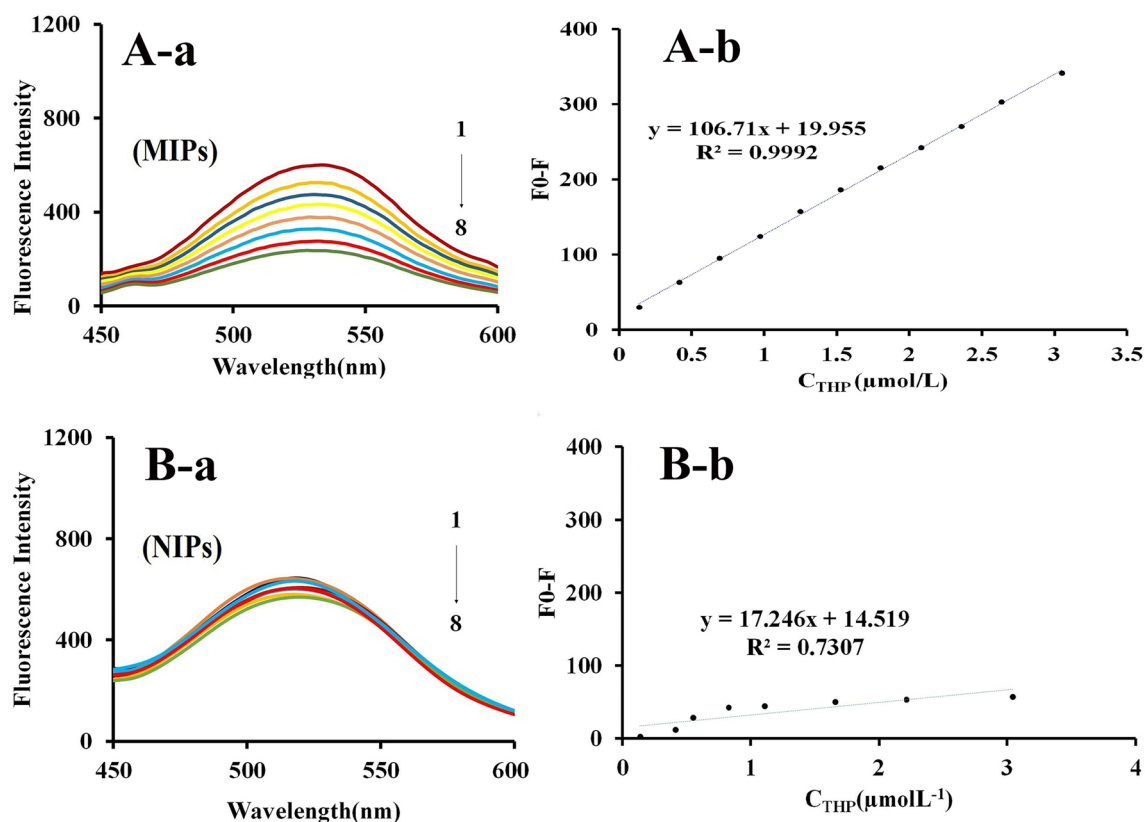


**Fig. 4** Fluorescence spectra of **A-a** QDs-MIPs, and **B-a** QDs-NIPs in the presence of different concentrations of THP ( $0\text{--}3.05\ \mu\text{mol L}^{-1}$ ); the obtained calibration curves for the QDs-MIPs

(**A-b**) and QDs-NIPs **B-b** at the optimal conditions with different concentrations of THP as ( $0.28\text{--}3.05\ \mu\text{mol L}^{-1}$ )

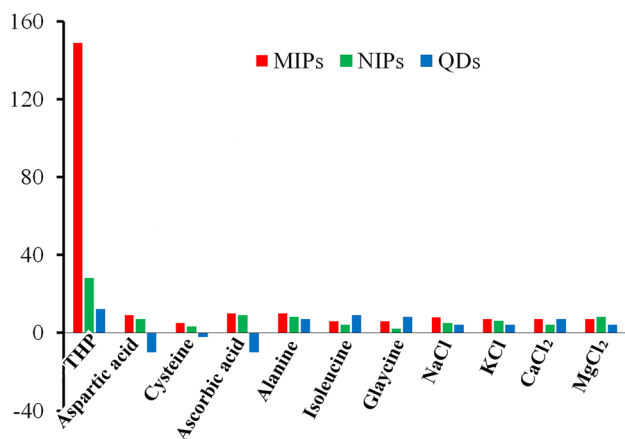


**Fig. 5** The responses of QDs-MIPs, QDs-NIPs, and QDs to THP ( $1.0\ \mu\text{mol L}^{-1}$ ) and different species ( $1.0\ \text{mmol L}^{-1}$ )

The obtained values (Table 1) confirm the applicability of the novel optical sensor for the measurement of THP in plasma samples.

**Table 1** Test of the applicability of the optical sensor for real sample analysis

Plasma sample	THP added ( $\mu\text{mol L}^{-1}$ )	THP found <sup>a</sup> ( $\mu\text{mol L}^{-1}$ )	Recovery%
1	1.00	$0.97 \pm 0.04$	97
	2.00	$1.81 \pm 0.07$	90
2	0.50	$0.54 \pm 0.04$	108
	1.00	$0.91 \pm 0.05$	91

<sup>a</sup>Average values for 3 determination  $\pm$  the standard deviations

## Conclusion

Incorporation of TGA-CdTe QDs into MIPs was employed as a selective and sensitive sensor for the determination of the THP for the first time. In this paper, the selectivity of the molecular imprinting technique and advantages of QDs were combined. The fabricated sensor showed strong fluorescence due to the presence of the QDs and high selectivity for THP due to specific cavities that are matching to the template molecule (THP) in form, size,

**Table 2** Comparison of analytical data for the determination of THP with spectrofluorimetric methods

Methods	LDR ( $\mu\text{mol L}^{-1}$ )	LOD ( $\mu\text{mol L}^{-1}$ )	Ref.
Chemiluminescent immunoassay	1.0–220	1.0	[22]
Fluorimetry based on aminopurine-modified abasic-site-containing duplex DNA	5–20	–	[23]
Fluorimetry based on RNA aptamer and graphene oxide	1–100	0.15	[24]
Fluorimetry based on DNA aptamer and silver nanoclusters	–	1.8	[25]
Fluorimetry based on a DNA duplex aptamer and a fluorescent ligand	1.0–32.5	1.1	[26]
Fluorescing based on molecular switches in combination with an RNA substrate	10–2000	–	[27]
Fluorimetry based on the MIPs-QDs	0.28–3.05	0.07	This work

and the binding sites. The sensor was successfully used for the measurement of THP in spiked plasma samples. The potential advantages of this nanosensor such as simplicity, selectivity, and sensitivity for the selective detection of various species will attract more attention for analysis application in the near future. Table 2 shows a comparison of analytical data of the proposed method and other spectrofluorimetric methods for determination of THP. As can be seen in this table, the limit of detection of the suggested method is comparable to the reported other methods.

## References

- H.R. Rajabi, M. Shamsipur, A.A. Khosravi, O. Khani, M.H. Yousefi, Selective spectrofluorimetric determination of sulfide ion using manganese doped ZnS quantum dots as luminescent probe. *Spectrochim Acta Part A Mol. Biomol. Spectrosc.* **107**, 256–262 (2013)
- M. Shamsipur, H.R. Rajabi, Pure zinc sulfide quantum dot as highly selective luminescent probe for determination of hazardous cyanide ion. *Mater. Sci. Eng. C* **36**, 139–145 (2014)
- M. Rutkowska, J. Płotka-Wasyłka, C. Morrison, P.P. Wiecek, J. Namieśnik, M. Marć, Application of molecularly imprinted polymers in an analytical chiral separation and analysis. *TrAC Trends Anal. Chem.* **102**, 91–102 (2018)
- L. Chen, J. Li, Recent advances in molecular imprinting technology: current status, challenges and highlighted applications. *Chem. Soc. Rev.* **40**, 2922–2942 (2011). <https://doi.org/10.1039/c0cs00084a>
- H.R. Rajabi, A. Zarezadeh, Development of a new chemically modified carbon paste electrode based on nano-sized molecular imprinted polymer for selective and sensitive determination of naproxen. *J. Mater. Sci. Mater. Electron.* **27**, 10911–10920 (2016)
- L.M. Madikizela, N.T. Tavengwa, H. Tutu, L. Chimuka, Green aspects in molecular imprinting technology: from design to environmental applications. *Trends Environ. Anal. Chem.* **17**, 14–22 (2018). <https://doi.org/10.1016/j.teac.2018.01.001>
- A.M. Piloto, D.S.M. Ribeiro, S.S.M. Rodrigues, C. Santos, J.L.M. Santos, M.G.F. Sales, Plastic antibodies tailored on quantum dots for an optical detection of myoglobin down to the femtomolar range. *Sci. Rep.* **8**, 1–11 (2018). <https://doi.org/10.1038/s41598-018-23271-z>
- J. Mayahi, H.R. Rajabi, Comparison study on separation of morin: ultrasound assisted molecularly imprinted polymeric nanoparticles-solid phase extraction versus solidification of floating organic-drop assisted dispersive liquid–liquid microextraction. *New J. Chem.* **41**, 14236–14245 (2017)
- E.E. Ferapontova, E.M. Olsen, K.V. Gothelf, Communication an RNA aptamer-based electrochemical biosensor for detection of theophylline in serum an RNA aptamer-based electrochemical biosensor for detection of theophylline in serum. *Communication* (2008). <https://doi.org/10.1021/ja711326b>
- S.R. El-Shabouri, S.A. Hussein, S.E. Emara, Colorimetric determination of theophylline and aminophylline with diazotized p-nitroaniline. *Talanta* **36**, 1288–1290 (1989)
- G.F. Johnson, W.A. Dechtiaruk, H.M. Solomon, Gas-chromatographic determination of theophylline in human serum and saliva. *Clin. Chem.* **21**, 144–147 (1975)
- E.P. Gil, H.T. Tang, H.B. Halsall, W.R. Heineman, A.S. Misiego, Competitive heterogeneous enzyme immunoassay for theophylline by flow-injection analysis with electrochemical detection of p-aminophenol. *Clin. Chem.* **36**, 662–665 (1990)
- M.C. Gutiérrez, A. Gómez-Hens, D. Pérez-Bendito, Stopped-flow fluorimetric determination of theophylline in pharmaceutical preparations. *Analyst.* **113**, 559–562 (1988)
- M. Sánchez-Cabezudo, J.M. Fernández-Romero, M.D. Luquede Castro, Fluorimetric-flow injection determination of theophylline based on its inhibitory effect on immobilized alkaline phosphatase. *Anal. Chim. Acta* **308**, 159–163 (1995)
- H. Jiang, K. Ling, X. Tao, Q. Zhang, Theophylline detection in serum using a self-assembling RNA aptamer-based gold nanoparticle sensor. *Biosens. Bioelectron.* **70**, 299–303 (2015)
- J. Wang, W. Cheng, F. Meng, M. Yang, Y. Pan, P. Miao, Hand-in-hand RNA nanowire-based aptasensor for the detection of theophylline. *Biosens. Bioelectron.* **101**, 153–158 (2018)
- A.A. Ensafi, N. Kazemifard, B. Rezaei, Development of a nano plastic antibody for determination of propranolol using CdTe quantum dots. *Sens. Actuators B Chem.* **252**, 846–853 (2017). <https://doi.org/10.1016/j.snb.2017.06.078>
- A.A. Ensafi, N. Kazemifard, B. Rezaei, Development of a selective prilocaine optical sensor based on molecularly imprinted shell on CdTe quantum dots. *Sens. Actuators B Chem.* **242**, 835–841 (2017). <https://doi.org/10.1016/j.snb.2016.09.175>
- M. Bagher, M. Shamsipur, S. Dehdashtian, H. Reza, Development of a selective and sensitive voltammetric sensor for propylparaben based on a nanosized molecularly imprinted polymer—carbon paste electrode. *Mater. Sci. Eng. C* **36**, 102–107 (2014). <https://doi.org/10.1016/j.msec.2013.11.021>
- J. Yang, M.-H. Wu, Z.-Z. Lin, Z.-Y. Huang, Detection of trace leucomalachite green with a nanoprobe of CdTe quantum dots coated with molecularly imprinted silica: via synchronous fluorescence quenching. *New J. Chem.* (2018). <https://doi.org/10.1039/c7nj04517d>

21. W. Zhang, X.W. He, Y. Chen, W.Y. Li, Y.K. Zhang, Composite of CdTe quantum dots and molecularly imprinted polymer as a sensing material for cytochrome c. *Biosens. Bioelectron.* **26**, 2553–2558 (2011). <https://doi.org/10.1016/j.bios.2010.11.004>
22. D.P. Malliaros, S.S. Wong, A.H.B. Wu, J. Campbell, H. Leonard, S. Houser, M. Berg, T. Gornet, C. Brown, Y.J. Feng, Quantitative determination of theophylline by an automated chemiluminescent immunoassay in serum and plasma: comparison to other methods of analysis. *Ther. Drug Monit.* **19**, 224–229 (1997)
23. M. Li, Y. Sato, S. Nishizawa, T. Seino, K. Nakamura, N. Teramae, 2-aminopurine-modified abasic-site-containing duplex DNA for highly selective detection of theophylline. *J. Am. Chem. Soc.* **131**, 2448–2449 (2009). <https://doi.org/10.1021/ja8095625>
24. K. Ling, H. Jiang, Y. Li, X. Tao, C. Qiu, F.-R. Li, A self-assembling RNA aptamer-based graphene oxide sensor for the turn-on detection of theophylline in serum. *Biosens. Bioelectron.* **86**, 8–13 (2016)
25. K.S. Park, S.S. Oh, H.T. Soh, H.G. Park, Target-controlled formation of silver nanoclusters in abasic site-incorporated duplex DNA for label-free fluorescence detection of theophylline. *Nanoscale* **6**, 9977–9982 (2014)
26. Y. Sato, Y. Zhang, S. Nishizawa, T. Seino, K. Nakamura, M. Li, N. Teramae, Competitive assay for theophylline based on an abasic site-containing DNA duplex aptamer and a fluorescent ligand. *Chem. Eur. J.* **18**, 12719–12724 (2012)
27. C. Frauendorf, A. Jäschke, Detection of small organic analytes by fluorescing molecular switches. *Bioorganic Med. Chem.* **9**, 2521–2524 (2001). [https://doi.org/10.1016/S0968-0896\(01\)00027-X](https://doi.org/10.1016/S0968-0896(01)00027-X)